Proc. Natl. Acad. Sci. USA
Vol. 93, pp. 2614–2619, March 1996
Physics

This contribution is part of the special series of Inaugural Articles by members of the National Academy of Sciences elected on April 25, 1995.

Colored diffraction catastrophes

M. V. BERRY AND S. KLEIN

H. H. Wills Physics Laboratory, University of Bristol, Tyndall Avenue, Bristol BS8 1TL, United Kingdom

Contributed by M. V. Berry, December 19, 1995

ABSTRACT **On fine scales, caustics produced with white light show vividly colored diffraction fringes. For caustics described by the elementary catastrophes of singularity theory, the colors are characteristic of the type of singularity. We study the diffraction colors of the fold and cusp catastrophes. The colors can be simulated computationally as the superposition of monochromatic patterns for different wavelengths. Far from the caustic, where the luminosity contrast is negligible, the fringe colors persist; an asymptotic theory explains why. Experiments with caustics produced by refraction through irregular bathroom-window glass show good agreement with theory. Colored fringes near the cusp reveal fine lines that are not present in any of the monochromatic components; these lines are explained in terms of partial decoherence between rays with widely differing path differences.**

Optical caustics are surfaces (in space) and curves (in the plane) where light rays are focused. They are as familiar as rainbows and the dancing bright lines of sunlight focused by water waves onto the bottoms of swimming pools. Caustics are the singularities of geometrical optics and can be classified mathematically as the elementary catastrophes (1–4) of singularity theory. In the plane, the classification gives two singularities: smooth caustic curves, which are "fold" catastrophes, and points where two fold caustics meet on opposite sides of a common tangent, which are "cusp" catastrophes. The classification contains those caustics that are stable under perturbations—e.g., of the optical arrangement giving rise to them—and so excludes unstable caustics, such as the isolated point focus.

On fine scales, which for monochromatic light are determined by the wavelength λ, the geometrical singularities are softened and decorated by diffraction fringes. Each type of caustic has its characteristic "diffraction-catastrophe" pattern. The fold diffraction catastrophe is Airy's function (5), and the cusp diffraction catastrophe is Pearcey's function (6); Fig. 1 shows the corrsponding intensity profiles.

Our purpose here is to extend the study of diffraction near caustics by exploring the fringes produced by white light, that is, by a superposition of wavelengths. Then the fringes are colored because the interference maxima for the different wavelengths occur at different places. (Here, we use the terms diffraction and interference interchangeably.) We find that these diffraction colors are surprisingly vivid and persist far into regions of large path lengths where it might be thought that the superpositions would give white. Apart from a dependence on the spectrum of the source of white light (here, assumed to be continuous), the colors are characteristic of the geometrical singularity, a fact that justifies the title of this paper. We present theoretical and experimental studies of the colored fold and colored cusp diffraction catastrophes.

In practice, the colors of caustics are often influenced by two effects that we shall ignore here. The first is physiological: with fringes whose spacing is a few arc minutes—i.e., near the limit of resolution of the eye—the colors disappear, leading to the apparently oxymoronic black-and-white fringes; this powerful illusion has been studied elsewhere (ref. 8, see also refs. 9–11). The second is refractive dispersion, which can color geometrical caustics even in the absence of diffraction; the most familiar refraction colors occur in the rainbow [although diffraction plays a large part too, especially for small raindrops (12, 13)]. For the fold, the balance between refraction and diffraction colors was studied in ref. 8 and quantified by a parameter a: with water, $a > 0$ describes maximum-deviation caustics with blue edges, such as those from thin irregular droplet "lenses", and $a < 0$ describes minimum-deviation caustics with red edges, such as rainbows.

Theory

As a function of coordinates $\mathbf{r} = x, y, \ldots = \{x_i\}$ and wavelength λ, the optical wavefunction $\psi(\mathbf{r},\lambda)$ that describes, for monochromatic light, the decoration of a given geometrical singularity is expressed in terms of a diffraction catastrophe function $\Psi(\xi, \eta, \ldots)$, where λ enters through the following scaling relation

$$\psi(\mathbf{r},\lambda) = \frac{C}{\lambda^{\beta}}\Psi\left(\left\{\frac{x_i}{\lambda^{\sigma_i}}\right\}\right), \qquad [1]$$

in which C is a constant (3). For the fold, Ψ is the Airy function:

$$\Psi(\xi) = 2\pi \mathrm{Ai}(\xi) = \int_{-\infty}^{\infty} dt \exp\left\{i\left(\frac{1}{3}t^3 + \xi t\right)\right\}, \qquad [2]$$

where the geometrical singularity is at $\xi = 0$, with $\xi < 0$ lit by two rays and $\xi > 0$ in shadow. For the cusp, Ψ is Pearcey's function:

$$\Psi(\xi,\eta) = \mathrm{P}(\xi,\eta) = \int_{-\infty}^{\infty} dt \exp\left\{i\left(\frac{1}{4}t^4 + \frac{1}{2}\xi t^2 + \eta t\right)\right\}. \qquad [3]$$

Here, the geometrical singularity is the curve

$$\eta = \pm \sqrt{\frac{4}{27}}(-\xi)^{3/2}. \qquad [4]$$

As already mentioned, this consists of two fold lines that meet with a common tangent at $\xi = \eta = 0$ on the symmetry (ξ) axis. "Inside" the cusp—e.g., near the negative ξ axis—there are three rays; "outside" there is one.

According to Eq. **1**, the emergence of the singularity in the geometrical optics limit $\lambda \to 0$ of vanishing wavelength is determined by the singularity exponents β and σ_i: the divergence of the intensity $|\psi|^2$ on the caustic is governed by β, and the diminishing size of the interference fringes in the direction

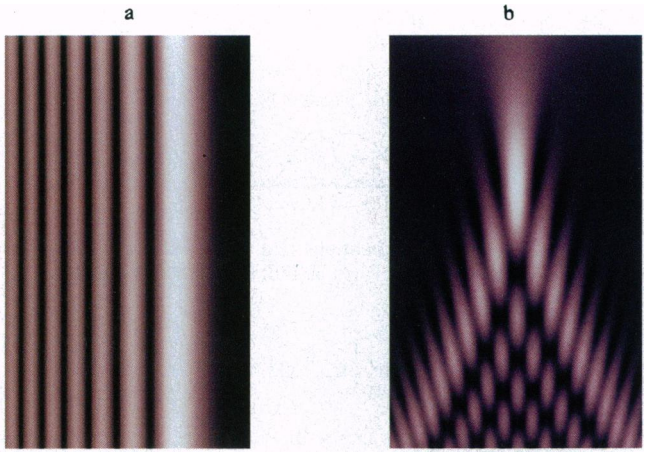

FIG. 1. Density plots of intensity of the monochromatic diffraction catastrophes for the fold (Airy function: $-10 \le \xi \le 3$) (*a*) and the cusp (Pearcey function: ordinate, $-9 \le \xi \le 2$; abscissa, $-10 \le \eta \le 1$) (*b*).

with coordinate x_i by σ_i. For the fold and cusp, these exponents are the following:

$$\text{fold; } \beta = 1/6, \sigma = 2/3$$

$$\text{cusp; } \beta = 1/4, \sigma_x = 1/2, \sigma_y = 3/4. \quad [5]$$

It follows that for the fold the intensity diverges as $\lambda^{-1/3}$ and the fringe size is proportional to $\lambda^{2/3}$. For the cusp, the fringes (cf. Fig. 1*b*) are more intense (diverging as $\lambda^{-1/2}$) and are thinner across the cusp—i.e., $\lambda^{3/4}$ in y—than along it—i.e., $\lambda^{1/2}$ in x.

For a white-light source with spectral distribution $S(\lambda)$, the intensity spectrum of the diffracted light at each field point $\mathbf{r}$ is

$$I(\mathbf{r},\lambda)=S(\lambda)|\psi(\mathbf{r},\lambda)|^2 \quad [6]$$

[in what follows, we will model $S(\lambda)$ by a black-body distribution with specified temperature—e.g., about 3300 K for a quartz–halogen lamp]. The theoretical prediction of the color at $\mathbf{r}$ requires the calculation of three tristimulus values in the system of the Commission International d'Éclairage (CIE) (14), namely,

$$U_i(\mathbf{r}) = \int d\lambda I(\mathbf{r},\lambda)\bar{u}_i(\lambda),$$

$$\text{where } U_i \equiv \{U,V,W\}, \bar{u}_i \equiv \{\bar{u},\bar{v},\bar{w}\}. \quad [7]$$

Here the $\bar{u}_i(\lambda)$ are the spectral tristimulus values that are derived from the mixture of primary colors that match a monochromatic light of wavelength λ and are related to the spectral responses of the three types of cone in the eye of a standard observer. In particular, the tristimulus value V represents the luminosity. Standard tabulations (15) give the $\bar{u}_i(\lambda)$ at 81 values across the visible range 380 nm $< \lambda <$ 780 nm, enabling the integral in Eq. **7** to be evaluated as a sum.

Calculations of the colored diffraction catastrophes from Eq. **7** were made by using the program MATHEMATICA. It was necessary to evaluate the integrals in Eqs. **2** and **3** for each of the 81 wavelengths across a grid of positions $\mathbf{r}$. For the fold, this was easy, first because the grid is one dimensional and second because MATHEMATICA contains an efficient and accurate routine for the Airy function. For the cusp, we calculated the Pearcey integral P in Eq. **3** over the grid $\{-9 \le \xi \le 2\},\{0 \le \eta \le 10\}$ with steps of 0.1 in ξ and η, and obtained intermediate values by interpolation between these 11,000 points. To compute P, we used numerical integration over a range $-t_{max} < t < t_{max}$, replacing the integral over $t > t_{max}$ by its asymptotic approximation based on expansion about t_{max} (see ref. 7 for this method of calculating P, and ref. 16 for a related method); for each (ξ, η), t_{max} was chosen so that all the real saddles of the integrand were captured in the numerical integration.

The diffraction colors were rendered by transforming the tristimulus values to RGB (red-green-blue) coordinates. This two-stage transformation is dependent on the display, and will be illustrated for an Apple Macintosh color monitor. The first stage is generated by a constant matrix, determined by the (measured) tristimulus values of the screen's red, green and blue:

$$\begin{pmatrix} R \\ G \\ B \end{pmatrix} = \mathbf{M}\begin{pmatrix} U \\ V \\ W \end{pmatrix}, \text{ where } \mathbf{M} = \begin{pmatrix} 3.78 & -1.72 & -0.57 \\ -1.20 & -2.06 & 0.05 \\ 0.03 & -0.19 & 0.76 \end{pmatrix}. \quad [8]$$

The second stage is the gamma correction to compensate for the (measured) nonlinearity of the screen:

$$\begin{pmatrix} R \\ G \\ B \end{pmatrix} \to \begin{pmatrix} U^{1/\gamma} \\ V^{1/\gamma} \\ W^{1/\gamma} \end{pmatrix}, \text{ where } \gamma = 1.9. \quad [9]$$

Simulations produced in this way are shown in Fig. 2*a* for the fold, and Fig. 3*a* for the cusp.

Asymptotic Colors

Colors persist deep into the interference regions of diffraction catastrophes, where it might be thought that the superposition of colors would give white. This can be explained and the calculation of tristimulus values (Eq. **7**) greatly simplified by an argument based on three observations. First, in this lit region, the diffraction-catastrophe intensities can be approximated (by using the method of stationary phase) by expressing Ψ as the sum of contributions from a few interfering rays and incorporating the wavelength scalings in Eqs. **1** and **5**. It is convenient to define the wavenumber by

$$k \equiv \lambda_Y/\lambda, \quad [10]$$

where $\lambda_Y \equiv 560$ nm is the wavelength of yellow light. For the fold, we have (17)

$$k^{1/3}\mathrm{Ai}^2(k^{2/3}x) \approx$$

$$\frac{1}{2\pi\sqrt{|x|}}\left(1 + \sin\left\{\frac{4}{3}k(-x)^{3/2}\right\}\right) \quad (x \ll 0) \quad [11]$$

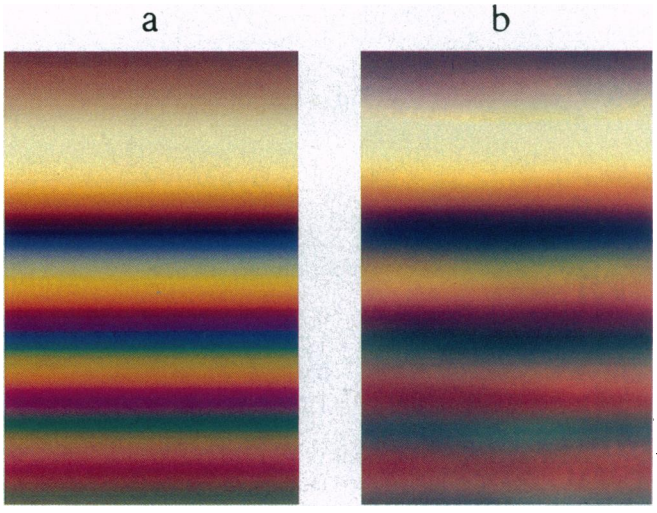

FIG. 2. Colors of the fold diffraction catastrophe. (*a*) Theoretical simulation ($-7.36 \le x/\lambda_Y{}^{2/3} \le 1.47$). (*b*) Experiment.

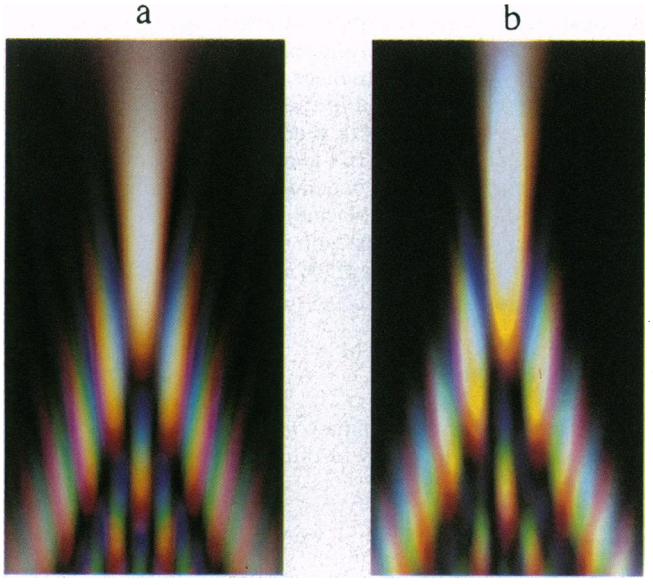

FIG. 3. Colors of the cusp diffraction catastrophe. (*a*) Theoretical simulation (ordinate, $-7.2 \le x/\lambda_Y^{1/2} \le 1.6$; abscissa, $-7.2 \le y/\lambda_Y^{3/4} \le 7.2$). (*b*) Experiment.

For the cusp, we have, in the interference region and near the symmetry axis (7),

$$k^{1/2}|\mathrm{P}(k^{1/2}x, k^{3/4}y)|^2 \approx \frac{1}{|x|\sqrt{2\pi}}\left(2 + 2\sqrt{2}\sin\left\{\frac{1}{4}kx^2\right\}\cos\left\{ky\sqrt{(-x)}\right\} + \cos\left\{2ky\sqrt{(-x)}\right\}\right) \quad (x \ll 0, |y| \ll |x|). \quad [12]$$

It will be important that in these approximate formulae all trigonometric functions have arguments proportional to k.

Second, when the integration variable in Eq. **7** is transformed from λ to k, the factors $S(\lambda)$, $u_i(\lambda)$ and the Jacobian $1/k^2$ can collectively be approximated with high accuracy by Gaussians. The approximations (Fig. 4) are

$$\left.\begin{aligned}\frac{1}{k^2}S(\lambda)\bar{u}(\lambda) &\approx a_{u1}\exp\left\{-(k-k_{u1})^2/2s_{u1}^2\right\} \\ &\quad + a_{u2}\exp\left\{-(k-k_{u2})^2/2s_{u2}^2\right\} \\ \frac{1}{k^2}S(\lambda)\bar{v}(\lambda) &\approx a_v\exp\left\{-(k-k_v)^2/2s_v^2\right\} \\ \frac{1}{k^2}S(\lambda)\bar{w}(\lambda) &\approx a_w\exp\left\{-(k-k_w)^2/2s_w^2\right\}\end{aligned}\right\}, \quad [13]$$

where, for a source with temperature 3300 K,

$$\left.\begin{aligned}a_{u1} &= 1.55, & k_{u1} &= 0.925, & s_{u1} &= 0.05 \\ a_{u2} &= 0.087, & k_{u2} &= 1.24, & s_{u2} &= 0.06 \\ a_v &= 1.05, & k_v &= 0.974, & s_v &= 0.07 \\ a_w &= 0.486, & k_w &= 1.22, & s_w &= 0.065\end{aligned}\right\} \quad [14]$$

Third, with the substitutions of Eqs. **12** and **13**, the integrations over k can be performed analytically (after the inconsequential extension of the range of integration to $k = -\infty$). We state the result for the tristimulus value V(x) for the coloured fold diffraction catastrophe:

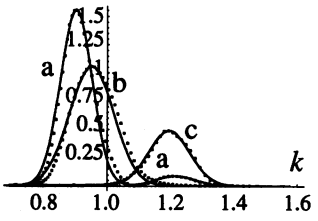

FIG. 4. Gaussian approximations (Eq. **13**) involving the spectral tristimulus values. (*a*) $\bar{u}$. (*b*) $\bar{v}$. (*c*) $\bar{w}$. Full lines, r.h.s. of Eq. **13**; dots, l.h.s. of Eq. **13**.

$$V(x) \approx \frac{a_v s_y}{2\sqrt{\pi|x|}}\left(1 + \sin\left\{\frac{4}{3}k_v(-x)^{3/2}\right\}\exp\left\{-\frac{8}{9}s_v^2(-x)^3\right\}\right) \quad (x \ll 0). \quad [15]$$

Analogous formulae hold for $U(x)$ and $W(x)$ and for the $U_i(x, y)$ for the cusp; in all the formulae, the trigonometric factors representing interference are damped by exponentials involving the widths s in Eq. **13**.

Now note that in Eq. **14** the largest width is s_v, corresponding to the tristimulus value V giving the luminosity of the fringes. Therefore, as $-x$ increases, that is, farther into the interference region near the caustic, the luminosity contrast will be damped (by the exponential in Eq. **15**) faster than the color contrast (whose damping is governed by the analogous exponentials in U and W). This is the explanation of the persistence of colors deep into the interference region. To illustrate this, we show the tristimulus values for the fold in Fig. 5, and, in Fig. 6*a*, a color rendering of this region, to be compared with the rendering of the luminosity shown in Fig. 6*b* and the monochromatic intensity shown in Fig. 6*c*. Note also that in Figs. 4 and 5 the predominantly blue tristimuli $\bar{w}$ and W are relatively faint (because of the low color temperature of the source). Therefore, in the deep-interference region, the predominant colors should alternate between red and green. That this is indeed the case for the fold can be seen in Fig. 6*a*; we postpone discussion of the cusp until the final section.

Experiment

Colored diffraction catastrophes were created in the far field of white light refracted by a pane of bathroom-window glass G (Pilkington's "Atlantic"); this is randomly corrugated on one side, with irregularities whose typical linear dimensions are 1 mm. The optical arrangement is shown in Fig. 7. From a tungsten–xenon lamp TX (equivalent to a 3300 K blackbody), light diverged from a pinhole P_1, was focused by a lens L (focal length 20 mm, whose purpose is to reduce the angular aperture of P_1 as seen from afar), and diverged again to strike a second pinhole P_2 which selected a region of about 1 mm^2 of G.

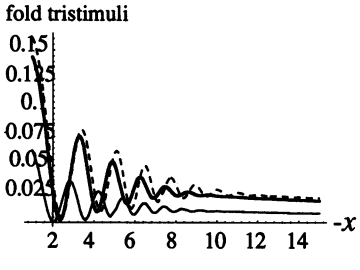

FIG. 5. Tristimulus values for the fold colored diffraction catastrophe in the interference region $-15 < x/\lambda_Y^{2/3} < -1$, calculated with the approximations of Eqs. **11**, **12**, and **13**. The dashed curve is $U(x)$, the bold curve is the luminosity $V(x)$, and the light curve is $W(x)$. Note that W is fainter than U and V and that the oscillations in V are damped faster than those in U.

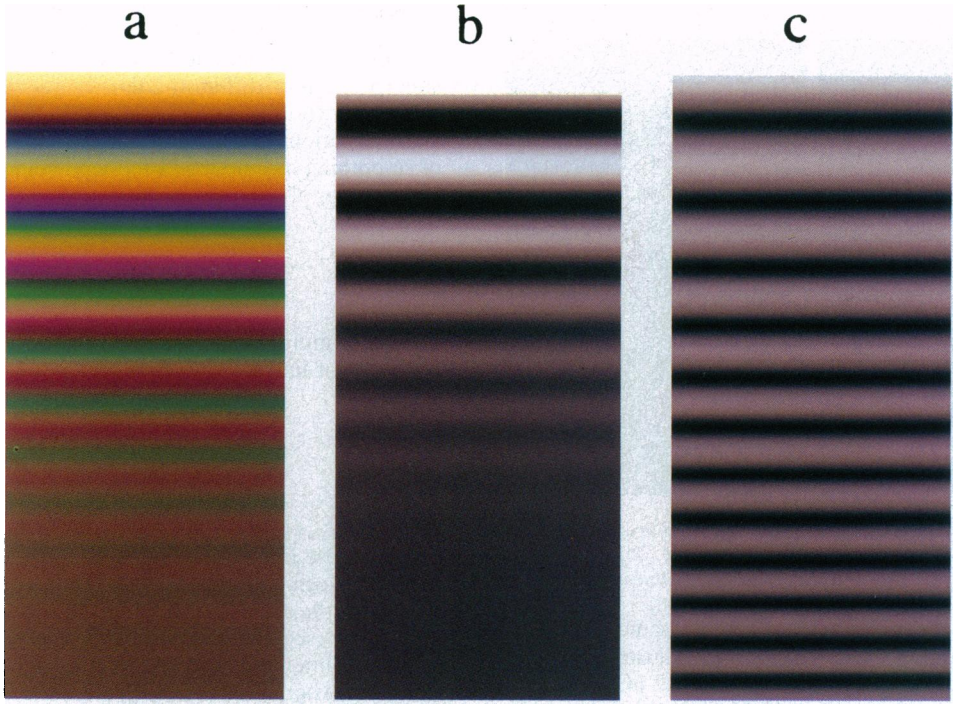

FIG. 6. (*a*) Colors of the fold diffraction catastrophe in the interference region $-15 < x/\lambda_Y^{2/3} < -1$. (*b*) Density plot of luminosity of the pattern in *a*, showing that the intensity contrast decays faster than the color contrast. (*c*) Density plot of the intensity $\mathrm{Ai}^2(x)$ of the monochromatic fringes.

The light focused by G forms a caustic surface whose far field (beginning about 10 mm beyond G) expands with distance, the typical angular size being 15°. Fringes, formed by interference between several refracted rays traversing the same region, decorate the caustic on fine scales; their typical angular size is 5–20′. The caustics were photographed without lenses by allowing the light to fall directly onto the film plane of a camera C. The form of the far-field caustics varied with the region of G that was selected; Fig. 8 is a typical example, showing the folds (smooth caustic curves) and cusps (cf. Eq. **4**) that are the stable singularities (1–4) in the plane. To obtain photographs showing details of these features, the regions containing them were magnified simply by moving C away from G. At the highest level of detail, the images were very faint: with the slide film Kodak Ektachrome 64T, we needed exposures of up to 15 min.

Because we are studying diffraction colors and neglecting refraction colors, it is important to work with caustics that are geometrically achromatic. In our bathroom-window glass experiments it was easy to achieve this by selecting the central region of the patterns; this procedure succeeds because the refractive spreading is proportional to the ray deflection and so is small near the forward direction. White cusps (accompanied by fold caustics showing strong refraction colors) were previously observed in light scattered backwards from oblate water drops (18) under conditions later shown (19) to be geometrically achromatic; however, the fringes near these cusps were too small to show diffraction colors.

In this way we obtained the detailed photographs of the fold and cusp colored diffraction catastrophes shown in Figs. 2*b* and 3*b*. These should be compared with the theoretical simulations shown in Figs. 2*a* and 3*a*. The color balance is not identical in each pair of pictures, perhaps, because the film we used incorporates a correction to bring the effective color temperature closer to that of daylight. To partially compensate for this, we normalized the raw monitor images (by using the program PHOTOSHOP) so that the colors of the brightest and

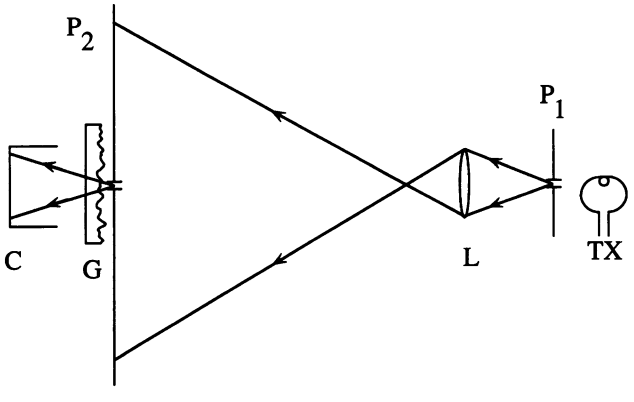

FIG. 7. Arrangement for observing colored diffraction catastrophes. C, camera; G, glass; L, lens; P_1 and P_2, pinholes 1 and 2; and TX, tungsten–xenon lamp.

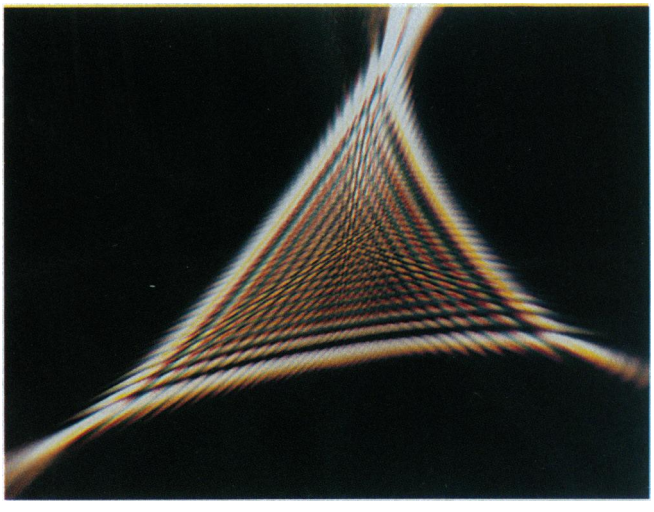

FIG. 8. Typical colored far-field caustic. Note the fine lines issuing from the cusps and crossing in the center of the pattern.

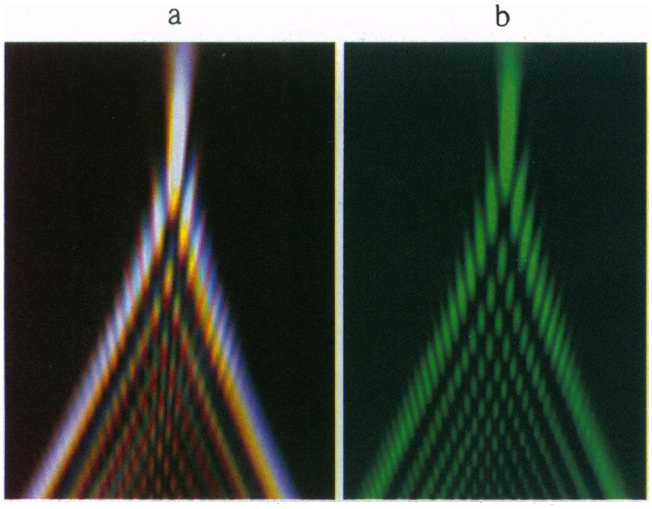

FIG. 9. (*a*) Colored cusp of Fig. 3*b*, at lower magnification, showing fine lines parallel to the symmetry axis. (*b*) Same caustic as in *a* photographed through a green filter, which causes the lines to disappear.

darkest parts of the theoretical images were the same as those in the experiments. It is possible to make further adjustments of the theoretical colors, to bring them closer to those in the experiments, but we did not do this. Overall, the agreement is rather good, with delicate observed tints being captured by the theory.

Lines of Partial Decoherence

A surprising feature of the colored cusp, visible in the "macroscopic" caustic of Fig. 8 but not in the magnifications of Fig. 3, is the set of fine lines parallel to the symmetry axis of the cusp. These can be clearly seen in the intermediate magnification of Fig. 9*a*. The lines can often be seen with the naked eye at night, in cusps produced from distant white lights by irregular raindrop "lenses" on spectacle lenses. What is surprising about the lines is that they disappear when the colored caustic is filtered into one of its monochromatic components, as in Fig. 9*b* (which is in good agreement with the theoretical monochromatic cusp of Fig. 1*b*). The lines are not present in any of the components and so must be artifacts of the superposition of different colors.

The key to understanding the lines is the observation that the integration over λ in Eq. **7** corresponds to a particular kind of smoothing or blurring of the monochromatic Pearcey function $P(\xi, \eta)$ of Eq. **3**, namely,

$$U_i(\mathbf{r}) = C^2 \int d\lambda \bar{u}_i(\lambda) S(\lambda) \frac{1}{\lambda^{1/2}} \left| P\left(\frac{x}{\lambda^{1/2}}, \frac{y}{\lambda^{3/4}} \right) \right|^2 . \quad [16]$$

This is a multiplicative (in λ) parametric smoothing along segments of lines obtained by scaling the caustic, namely,

$$\frac{\eta}{y} = \left(\frac{\xi}{x} \right)^{3/2} . \quad [17]$$

The length of the segments is determined by the limits λ_{min} to λ_{max} ($\approx 2\lambda_{min}$) of the visible spectrum (the functions u_i vanish outside these limits) and by the values x and y. Near the cusp point, the segments are short, and the smoothing is ineffectual; this is why the colored diffraction catastrophe is white near the cusp point (see also the final paragraph below).

In the interference region and close to the symmetry axis—i.e., where $y \ll (-x)^{3/2}$—the line segments of Eq. **17** are close to the ξ axis and parallel to it and get longer as x increases. The effect of smoothing along these lines is to reduce the contrast along x—i.e., parallel to the symmetry axis of the cusp—while leaving virtually unaffected the contrast across x. Thus, the lattice of interference maxima (Figs. 1*b* and 9*b*) near the negative x axis gets replaced by line fringes, as observed.

There is another way to regard this phenomenon of λ smoothing, in which the coherence of some fringes is destroyed but other fringes are preserved. Each point inside the cusp is reached by three rays, whose interference in monochromatic light gives the pattern of maxima and minima in Figs. 1*b* and 9*b*. If the rays have very different phases, the effect of λ smoothing will be to destroy the fringes by decoherence. If two of the rays r_1 and r_2 have a very small phase difference and

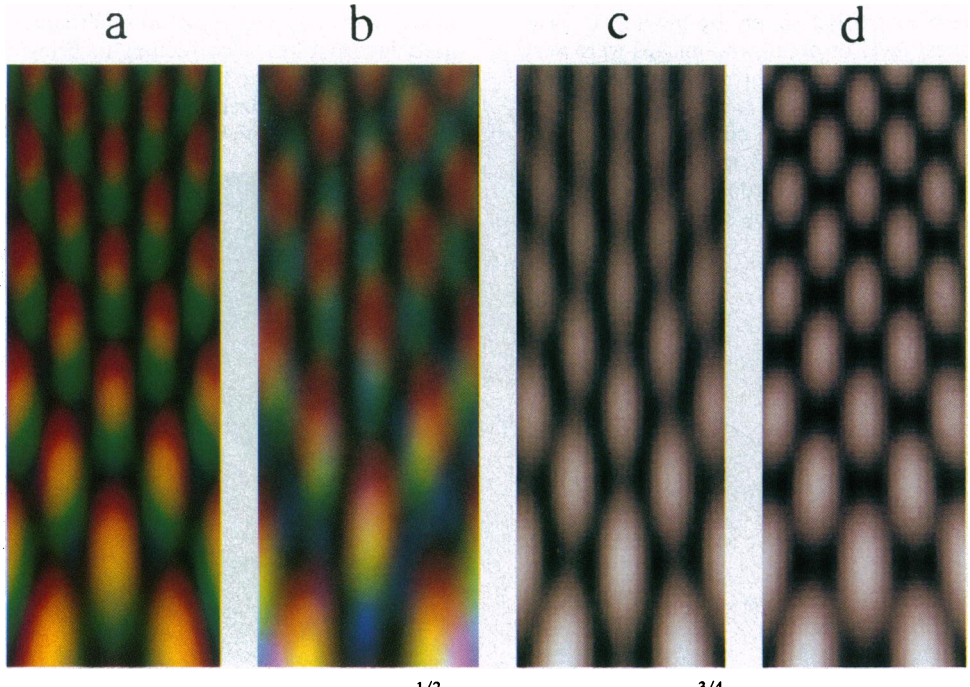

FIG. 10. Deep inside the colored cusp (ordinate, $4.3 \leq -x/\lambda_Y^{1/2} \leq 12$; abscissa, $-2.7 \leq y/\lambda_Y^{3/4} \leq 2.7$). (*a*) Theoretical colors. (*b*) Experiment. (*c*) Density plot of luminosity of coloured pattern. (*d*) Density plot of intensity of monochromatic pattern $|P(x, y)|^2$.

differ greatly in phase from the third ray r_3, then the fringes associated with the interference of r_1 and r_2 will be preserved, while that associated with their interference with r_3 will be destroyed. Precisely this partial decoherence occurs inside the cusp and near the axis; in Eq. **12**, the first term—i.e., 2—in the brackets represents the sum of the intensities of the three rays, the third term represents the interference between r_1 and r_2, and the second term (involving kx^2) represents their interference with r_3. It is now obvious that the effect of making r_3 incoherent with r_1 and r_2 is indeed to obliterate the fringes along x—i.e., to eliminate the second term in Eq. **12**—while preserving those across x.

If this explanation is correct, extension of the theoretical calculation of the colored cusp diffraction catastrophe of Fig. 3*a* to include more of the interference region deep inside the cusp should reveal the lines. As shown in Fig. 10*a*, it does, and the lines agree with those seen experimentally (Fig. 10*b*). Moreover, the lines are also present in the luminosity of the patterns (Fig. 10*c*) but not, of course, in the monochromatic intensity (Fig. 10*d*).

It should be noted that this one-dimensional λ-induced smoothing along the lines specified by Eq. **17** is very different in its effects from the more familiar two-dimensional smoothing produced, for example, by degrading the spatial coherence of a monochromatic source, such as a laser. This latter smoothing does not produce the fine axial lines but simply blurs the whole pattern, as the simple experiment of defocusing a slide of Fig. 1*b* or Fig. 9*b* shows.

Finally, observe that in Fig. 9*a* not only is the principal maximum at the cusp point white but the maxima far along the fold lines emanating from the cusp are white too; the first few maxima on the fold are colored. To explain these facts, we note that on the fold lines two of the three rays are degenerate, and therefore their contribution gives white wherever the third ray is negligible, and this is the case far from the cusp. At the cusp itself, all three rays are degenerate and so, as we have seen already, the principal maximum is white. Only for the first few maxima along the fold is the third ray bright enough for its phase difference with the other two to generate colors.

We thank Professor J. F. Nye for several helpful suggestions.

1. Arnold, V. I. (1986) *Catastrophe Theory* (Springer, Berlin), 2nd Ed.
2. Berry, M. V. (1981) in *Les Houches Lecture Series Session 35*, eds. Balian, R., Kléman, M. & Poirier, J-P. (North-Holland, Amsterdam), pp. 453–543.
3. Berry, M. V. & Upstill, C. (1980) *Prog. Opt.* **18,** 257–346.
4. Poston, T. & Stewart, I. (1978) *Catastrophe Theory and Its Applications* (Pitman, London).
5. Airy, G. B. (1838) *Trans. Cambridge Philos. Soc.* **6,** 379–403.
6. Pearcey, T. (1946) *Phil. Mag.* **37,** 311–317.
7. Berry, M. V., Nye, J. F. & Wright, F. J. (1979) *Philos. Trans. R. Soc. London* **A291,** 453–484.
8. Berry, M. V. & Wilson, A. N. (1994) *Appl. Opt.* **33,** 4714–4718.
9. Mullen, K. T. (1985) *J. Physiol. (London)* **359,** 381–400.
10. Hilz, R. & Cavonius, C. R. (1969) *J. Opt. Soc. Am.* **60,** 273–277.
11. Hilz, R., Huppman, G. & Cavonius, C. R. (1974) *J. Opt. Soc. Am.* **64,** 763–766.
12. Buchwald, E. (1943) *Ann. Phys.* **43,** 488–493.
13. Kubesh, R. J. (1992) *Am. J. Phys.* **60,** 919–923.
14. Travis, K. T. (1991) *Effective Color Displays: Theory and Practice* (Academic, London).
15. Kaye, G. W. C. & Laby, T. H. (1973) *Tables of Physical and Chemical Constants* (Longman, London), 14th Ed.
16. Connor, J. N. L. & Curtis, P. R. (1982) *J. Phys. A* **15,** 1179–1190.
17. Abramowitz, M. & Stegun, I. A. (1972) *Handbook of Mathematical Functions* (Natl. Bureau of Standards, Washington, DC).
18. Simpson, H. J. & Marston, P. L. (1991) *Appl. Opt.* **30,** 3468–3473.
19. Nye, J. F. (1992) *Proc. R. Soc. London* **A438,** 397–417.